Evaluation of data acquisition techniques and workflows for Scan to BIM

Maarten Bassier, Meisam Yousefzadeh and Bjorn Van Genechten

K.U. Leuven Faculty of Engineering Technology, Technology Campus Ghent

Maarten.bassier@kuleuven.be, m.yousefzadeh@utwente.nl, Bjorn.VanGenechten@leica-geosystems.com

KEY WORDS: Surveying, Scan to BIM, Terrestrial Laser scanning, Building, Mobile Mapping

ABSTRACT:

With the increasing popularity of as-built Building Information Modelling (BIM) for existing buildings, the demand for highly accurate and dense point cloud data is rising. However, the current data acquisition methods are labor intensive and time consuming. Among other factors, the use of total station measurements to establish survey control, is a major cost behind data acquisition workflows. Over the recent years, there have been major innovations in the fields of surveying and robotics, such as the development of Indoor Mobile Mapping systems (IMMS). With these technological advancements, more cost-effective workflows for capturing existing buildings can be realized.

In this paper, several state-of-the-art data acquisition techniques and workflows are discussed for Architectural, Engineering and Construction (AEC) industry buildings. Furthermore, a workflow is proposed with a standalone terrestrial laser scanner capturing data in high overlap, using loop-closure and optimization algorithms to guaranty accuracy. Real life test cases of AEC industry buildings are presented, proving that the proposed workflow can provide highly dense point cloud data within project specifications more efficiently.

1.   Introduction

1.1.   Motivation

Over recent years, the demand for accurate Building Information Models (BIM) of existing buildings has increased. These as-built BIM's are often required to be modelled up to Level-of-detail (LOD) 300 [1], and up to Level of Accuracy (LOA) 30 [2,3]. To provide this data, high resolution and high accuracy point cloud data is required.

Despite rapid innovation over the last decade, the creation of a highly accurate dense point clouds for mid-to-large scale Architectural, Engineering and Construction (AEC) buildings remains a labor intensive process [4]. One of the main reasons for this inefficiency is the lack of innovation in survey workflows. Currently, the most popular instrument for the acquisition of point cloud data is a terrestrial laser scanner. In current workflows, a terrestrial laser scanner, placed on a tripod, is used to make scans on multiple locations [5]. The individual point clouds are tied together using artificial targets that are spread throughout the scene. Each point cloud contains at least three or more targets. In addition, the targets are also measured with total stations to establish survey control. While this workflow is highly accurate, it is a costly and time consuming process. The driving costs in time and money are the use of total stations, which require additional personnel, the static approach, which lowers the data acquisition speed, and the manual registration, which increases post-processing time. In addition, the establishment of the survey control network by total station demands certain know how, requiring expensive survey specialists.

With the development of new survey techniques, improved registration algorithms and the rapid advancement of terrestrial laser scanners over the past several years, survey workflows will also start to change. We believe that, when combined properly, these innovations can result in more cost-effective workflows compared to traditional procedures.

2.   Related work

Several researchers have published findings on data acquisition solutions for building modelling. Generally, the emphasis has been on the automated 3D reconstruction of indoor environments [5–14]. While many approaches have proven to be successful, most solutions are limited to small scale data (e.g. a hallway, a room, etc.). Papers discussing the mapping of larger data sets, mainly focus their research on mobile solutions. One of the most prominent publications has been the comparison of IMMS compared

to Terrestrial laser scanning (TLS) in terms of accuracy and acquisition speed [5]. In this research, both the iMMS of Viametris [15] and the ZEB1 from CSIRO [16] are discussed, concluding that IMMS might have a significant impact on future workflows, but currently lack sufficient accuracy. Also, the University College London (UCL) presented a report with the test case of a Scan-to-BIM project [4]. Data acquisition was performed using a terrestrial laser scanner along with total station measurements. Their research concluded that traditional survey workflows were inefficient and that iMMS might provide a solution. Several other papers have been presented on the ZEB1, describing the system as a solution for low accuracy applications [16,17]. Similar to the Viametris, findings have been reported for several other trolley based systems [36,37]. Another solution is the integration of several 2D laser scanners and other sensors in a backpack [18,19], providing a fast and hands free approach. Other LIght Detection And Ranging (LIDAR) integrated approaches have similar results [21]. A lot of research is being performed on the integration of RGB-D cameras like the Microsoft Kinect for indoor mapping [6–8,11,12,21]. While projects like Google Tango [35], Kintineous [7] and Kinfu [10] succeed in mapping larger areas, the integrated sensors lack the accuracy and range for building mapping. Photogrammetric approaches are being explored as well [23], but generally require additional information from LIDAR or RGB-D.

3.   AEC buildings

The focus of this research is on the data acquisition of AEC building e.g. entire airports, hospitals, office buildings, schools, etc. These buildings consist of multiple structures, with several floors, covering several ten thousands of square meters of useful space, and are filled with repetitive objects. Given these conditions, several problems arise for the point cloud acquisition.

One of the major problems of Scan to BIM is data occlusion. Even with high resolution survey data, occluded zones like the interior of walls, floors and ceilings, cannot be avoided. However, a lot of occlusion is caused by the sensors position. Scan to BIM algorithms are forced to make assumptions about these zones, which often lead to misinterpretation. To minimize data occlusion, data coverage should be maximized, and thus, the sensor should be able to access all kinds of spaces.

Another major factor is the resolution of the survey data. Different zones and objects require a certain data resolution in order to be modelled correctly. However, with data resolution inversely proportional to the acquisition speed, the resolution/acquisition time ratio has to be optimized. Acquisition workflows should aim for maximizing speed with a minimum of misinterpretation.

Also the type of point cloud influences Scan to BIM efficiency. Different survey systems provide varying types of point clouds. Reconstruction algorithms preferably work with structured data, for computational efficiency.

The possibility of capturing RGB/grayscale imagery in addition to the LIDAR data is a major asset in scene interpretation. While modelling algorithms are not yet integrated with RGB/grayscale imagery based approaches, modelers find them invaluable for scene interpretation.

There is also the problem of similarity. These type of AEC buildings tend towards great similarity across different rooms and floors. Since most Simultaneous Localization And Mapping (SLAM)[39] or automatic registration algorithms rely on the unicity of environments throughout the project, similarity can cause major confusion in the localization process .

4. Data acquisition techniques and workflows

4.1. Terrestrial laser scanners

Terrestrial laser scanners are advancing rapidly. Over the course of several years, acquisition times have dropped from over half an hour to only a couple of minutes for each scan. This allows for more setups, resulting in larger data coverage. With data acquisition speeds up to a 1,000,000 HZ, weight down to 5-10kg, increased accuracies to up to 6mm/100m, terrestrial laser scanners look stronger than ever.

Scanning speed can be increased even more using Multiple-Pulses-in-Air (MPiA) technology [24] in pulse-based Time of Flight (TOF) laser scanners. Also, the implementation of full waveform analysis has led to more accurate data, effectively removing mixed edge pixels and capturing multiple returns from the laser beam [25].

Figure 1: Leica ScanStation P20 image from *http://www.leica-geosystems.com/*

Furthermore the capability to capture RGB data along with LIDAR data is an important asset. While RDB and LIDAR acquisition are currently separated, simultaneous acquisition of RGB and LIDAR is an ongoing research [26,27].

However, High cost, low rate of data acquisition and the post-processing form major drawbacks of these systems. Also, this technique is among the most expensive scanning technologies. Because of project similarity, some constraints have to be manually provided to avoid misalignment. Currently, most semi-automated registration softwares use a minimum of manual constraints as a basis for their automated constraint algorithms. However, these algorithms match all clouds in the project. This causes high computational complexity :

Figure 2: FARO Focus3D X330 image from *http://www.faro.com/*

$$\text{Constraints} = \sum_{n=1}^{clouds}(\text{n} - 1) \tag{1}$$

E.g.: A 400 scan project generates up to 79,800 constraints

As a side effect of the high resolution data and the many setups, terrestrial laser scanners generate enormous amounts of data. It is not uncommon for a project to contain several hundreds of clouds, consisting of tens of millions of points, resulting in a final points cloud housing billions and trillions of points. Most software packages have problems processing this amount of data, so the data has to be partitioned manually. However, Data Base Management Systems (DBMS) are proposed [28] as a solution, offering efficient storage and visualization. Most commonly, intelligent sparse voxel octrees [29] are introduced that efficiently process the data in contrast to normal data bases.

Terrestrial laser scanning is a multidisciplinary employed system for scanning operations. With its simple tripod setup, the instrument can enter any area inside and outside of AEC buildings, and provide high accurate, high resolution point cloud data at increased ranges. For now, terrestrial laser scanners are the only devices capable of providing a standalone solution for the capturing of Architectural, Engineering and Construction projects.

4.2. Mobile mapping systems (MMS)

One of the most interesting innovations in surveying of the last decade has been the development of mobile data acquisition devices. Stepping away from traditional static setups, these techniques combine several sensors into a mobile device, allowing them to dynamically survey the scene.

Mobile mapping systems can be separated in two categories: Indoor and outdoor. The difference between the two categories is the availability of GPS. A typical outdoor mobile mapping systems like a drone or a mobile mapping vehicle mainly determines it's position using GNSS signals. Localization is enhanced using Inertial measurement units (IMU), wheel odometry or other sensors. For indoor applications, such as Scan to BIM, where GNSS signals are unavailable, mobile mapping systems have to determine their position differently. Most indoor mobile mapping systems (IMMS) use Simultaneous Localization And Mapping (SLAM) algorithms to compute their trajectory. Originating from the robotics industry, SLAM is a process that allows a robot to simultaneously survey its environment, and track its own location within that environment [30].

Dynamic approaches have considerable advantages over static solutions in Scan to BIM projects. Indoor mobile mapping systems have greatly increased scan times, allow more data coverage and often have real time registration, effectively reducing post-processing time. Several dynamic devices even have online feedback, providing the user with an overview of the map while scanning.

However, IMMS trade increased acquisition speed for reduced accuracy. Where terrestrial laser scanners achieve up to several millimeters accuracy, IMMS can only provide several centimeters accuracy. This is caused by the use of small lightweight sensors, reducing resolution, range and accuracy. Also, SLAM algorithms are prone to drift, can lose tracking in featureless zones, and will fail in zones with high similarity.

Several systems have been developed over recent years. The two main approaches of SLAM implemented techniques are handheld devices and trolley based devices, both having their advantages and disadvantages. In the following section, the ZEB1 from CSIRO [15,17], the IMMS from Viametris [15] and the M3 mapping trolley from NavVis [36] will be discussed along with their capability for Scan to BIM applications.

ZEB1

Figure 3: ZEB1 device image from
http://www.3dlasermapping.com/

The ZEB1 or Zebedee is a handheld device developed by the Australian research group CSIRO in 2012. It consists of a spring mounted 2D laser scanner and IMU (figure 3). The laser used in this system is a Hokuyo UTM-30LX: a 2D ToF laser with a range of 30m, acquisition speed of 40,000Hz and an accuracy approximately 1cm/10m [31]. The industrial grade IMU used is a MicroStrain 3DM-GX2, a MEMS based IMU with an output rate of 100Hz. Accuracies of 2.5cm have been reported [5].

As the operator periodically nods the head, a small 3D point cloud is extracted using the IMU localized laser beams. These clouds are registered together using an open-loop SLAM algorithm, enhanced to deal with the irregular motions of the sensor head [32].

During data acquisition, the operator is adviced to make as many loops as possible throughtout the scene. This will allow the post-processing loop-closure algorithm to enhance the devices trajectory, reducing drift. For best practices, the operator should therefor start in the center of the project, venturing outwards and returning to the center over and over again. Also, in order to avoid loss of track, the sensor requires a suffcient amount of 3D landmarks [9]. This indicates the scan head should be nodding at all times, and featureless scenes should be avoided.
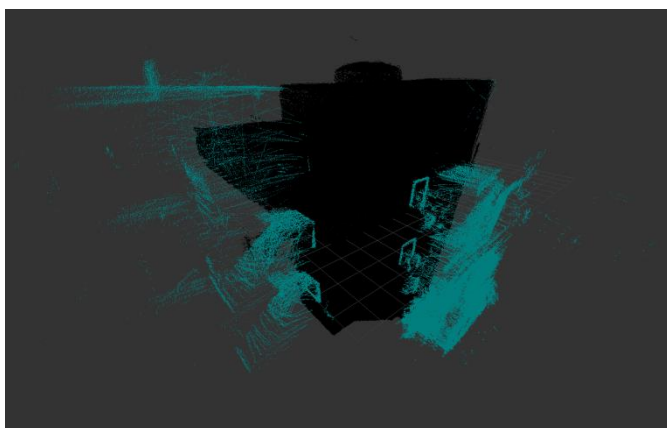

Figure 4: ZEB1 Demo Building on Campus. Black is correct data, Cyan data is noise caused by windows

The benefits of this system are the low cost, the fast and easy data acquisition, the automated processing and the employability in all areas. However, there are several disadvantages to this system. First, there is the lack of imigary or panoramic imigary, making scene interpretation hard. Second, the system provides non-structured low resolution data, causing higher computational complexity and misinterpretation for algorithms. Third, the

Hokuyo UTM-30LX does not include full waveform analysis, resulting in noisy data compared to traditional laser scanning (figure 4). Last, the generated drift will exceed project requirements in bigger projects.

IMMS from Viametris

The IMMS is a trolley based system designed by Viametris, a French spin off founded in December 2007. It consists of three 2D laser scanners, a panoramic camera and an onboard computer, mounted on a kinematic platform. One laser, a Hokuyo UTM-30LX is fixed in a horizontal position, and two Hokuyo UTM-30LX-EW [33] are fixed in vertical positions. The latter are used for mapping since they are implemented with full waveform analysis. The used camera is a Ladybug3, a 12MP spherical camera that can stream up to 15 FPS. Accuracies of 2.5cm have been reported [5].

As the operator pushes the cart throughout the scene, the horizontal Hokuyo feeds the open SLAM algorithm. The 2 vertical lasers are placed under an angle, ensuring data coverage. The on board computer gives online feedback about the SLAM results.

Major benefits of the system is the increased resolution and the capability of capturing imagery, making it an outstanding device for the creation of virtual tours. The structured data also benefits computational complexity, while the online feedback aids with user interaction.

Figure 5: Viametris image from *http://www. viametris.com/*

However, the Viametris has several downsides. First, there is the limited employability. Since the localization is in 2D, the system assumes the ground to be perfectly horizontal. There for, the device cannot be used in anything other than flat terrain. Just like the ZEB1, the device is also prone to drift and project similarities. For these reasons, the Viametris IMMS cannot be used as a standalone device for the capturing of AEC buildings.

M3 from NavVis

The M3 is a trolley based system developed by the German spin-off NavVis in 2013. It consists of three 2D laser scanners (Hokuyo UTM-30LX), an IMU, an HDR panoramic camera, WiFi sensors, magnetic field sensors and an onboard computer mounted on a kinematic platform. The setup is similar to that of the IMMS of Viametris, with the addition of multiple sensors to enhance the SLAM localization.

The graph-based SLAM algorithm is not only realized by the 2D laser input from the Hokuyo, but also from panoramic images, WiFi measurements [34], Magnetic field measurements and IMU input. The different sensor measurements are combined into a powerful positioning algorithm that is more robust to drift and project similarity. Also, it doesn't need the assumption of a perfectly horizontal floor. The HDR imagery also allows data acquisition in poor lighting conditions, increasing consistency of the data.

Figure 6: iMMS from Navvis image from *https://www. navvis.com/*

The accompanied software allows fully automated post-processing including non-linear optimization and loop-closure. Furthermore, 2D floor plans are automatically extracted and an intelligent cloud based engine based on a sparse voxel octree is provided to easily access the data [36].

The disadvantages of the system remain sensor noise and limited range caused by the Hokuyo sensors. Also the trolley cannot access all terrains e.g. staircases. The M3 cannot be used as a standalone solution for entire buildings, but combined with other devices, it has great potential for indoor mapping.

4.3.   Comparison

	Terrestrial laser scanning	Zebedee	Viametris	Navvis
Cost	High/Very High	Low	High	High
Speed	Low	Very high	Very high	Very high
Accessibility	High	Very High	Low	Low
Data quality	High/Very high	Low	Low	Low
Structured data	Yes	No	Yes	Yes
Color	RGB/HDR	No	RGB	HDR
Simultaneous capture of RGB and LIDAR	No	/	Yes	Yes
Range	100m+	<25m	<25m	<25m
Local Accuracy	6mm/100m	3cm/30m	3cm/30m	3cm/30m
Global Accuracy	/	<2.5cm	<2cm	<2cm
Multidisciplinary	High	Moderate	Low	Moderate
Automated Registration	Semi	Yes	Yes	Yes
Stand-alone solution	Yes	No	No	No

Table 1: Comparison of TLS and IMMS

With several system investigated, we state that while terrestrial laser scanning is the slowest and most expensive technique, it still has the edge over dynamic acquisition devices in terms of accuracy and multidisciplinarity (table 1). With the ongoing developments in the fields of the simultaneous capturing of RGB and LIDAR, acquisition speed, HDR imaging, automated registration, etc. terrestrial laser scanning will remain one of the prominent techniques for Scan to BIM projects.

5.   Proposed workflow

The current laser scanning workflow is outdated. The use of total stations to establish survey control is a major time consuming factor. We believe that, with the developments in registration algorithms and data accuracy, the use of total stations have become unnecessary to acquire project specifications.

We propose a revised workflow with only terrestrial laser scanner measurements and cloud to cloud registration. Scanning with high overlap will provide a good alignment and a tight network that can be optimized. Furthermore, creating as many loops as possible throughout the projects will enable loop-

closure, greatly reducing drift accumulated in the registration process. In the case of geolocated projects, GPS measurements can be added to georeference the data and increase accuracy.

5.1.   Test Results

To evaluate the approach, two in-the-field test cases are presented. The projects will be conducted using both the initial workflow and the revised one. By comparing total station measurements with the cloud to cloud registered data, an overall accuracy can be determined for the new workflow.

Mid-scale test site

The first test site is the east passage of the central station in Amsterdam. It roughly consists of a rectangle of 70 x 40 x 4m (figure 7), and houses 3 major sections. Project specifications prescribe an overall accuracy of the point cloud of 1.5cm, according to LOA30 [3]. A reference network was established by an external surveying company using total station measurements (figure 8).
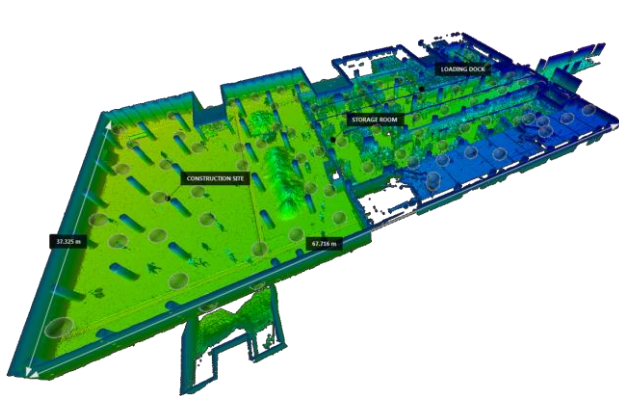
Figure 7: Project overview, scan locations
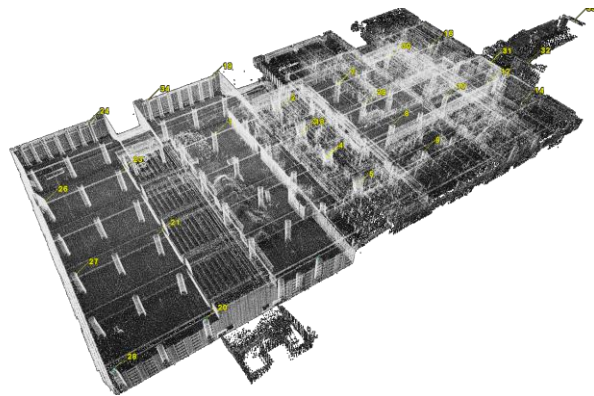
Figure 8: Project overview, control points

Data acquisition and processing

The laser scan measurements were conducted using a Faro Focus3D S120 laser scanner. 98 scans were acquired, each about 5-10m from each other (figure 7), to minimize occlusion zones. Each scan took 1.27 minutes, measuring 10,900 million points. The site was scanned under 4 hours, resulting in a total point cloud of approximately one billion points. No color was acquired during acquisition. The data processing was performed using Cyclone registration software from Leica Geosystems. 97 manual constraints had to be provided, after which 1400 constraints were automatically found. 7 hours of post-processing was timed, including 4 hours of manual labor.

The control measurements were conducted by a two man team. 33 targets were materialized throughout the scene, using 29 setups, providing an accuracy of 2mm on each point (figure 8). Acquisition and processing was performed in under a day.

Comparison

In order to calculate the gained efficiency, a comparison is made of the total processing time of both workflows. Table 2 shows that the proposed workflow is at least 39% faster. Also, the costs are greatly reduced since one operator can scan the entire project and no targets have to be extracted from the clouds.

	Acquisition time [h]	Post processing [h]	Total [h]
Traditional workflow			
• Point cloud acquisition	4	7	11
• Total station measurements	4	3	7
Proposed workflow			
• Point cloud acquisition	4	7	11
Saved Time	**4**	**3**	**7**
Efficiency	**50%**	**30%**	**39%**

Table 2: Comparison of both workflows in terms of acquisition speed and post-processing time

To evaluate the workflows in terms of accuracy, the laser scan data will be matched to the control network. This is performed using artificial targets known in both the scan data and the total station

network. The targets are acquired statistically from the cloud with an accuracy of 2mm. The survey measurements will be used as the benchmark and the point cloud measurements as the test group. Using a least squares approach in Matlab, the best fit transformation was calculated from the point clouds to the survey model. The error values between the two data sets are presented in table 3 and figure 10.
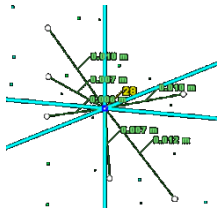
Figure 9: Statistical extraction of scanned targets

$$X' = P\,X \tag{2}$$

$$P = \begin{bmatrix} \mathbf{R} & \mathbf{t} \\ \mathbf{0}^\mathsf{T} & 1 \end{bmatrix} \tag{3}$$

	X	Y	Z
% within specification (1.5cm)	100%	100%	100%
Biggest error [m]	0,0068	0,0079	0,0120
RMSE [m]	0,0025	0,0028	0,0051

Table 3: Comparison between cloud to cloud registration and the survey network first test case

The deviation from the cloud to cloud registration compared to the survey network is several millimeters. These errors are even smaller considering the total station, the laser scanning and the target extraction accuracy. All points are within project specifications. However, the error in z direction is higher than in other directions. By plotting the deviations on the point cloud, it is revealed that the project is slightly bending upwards (figure 10, 11).
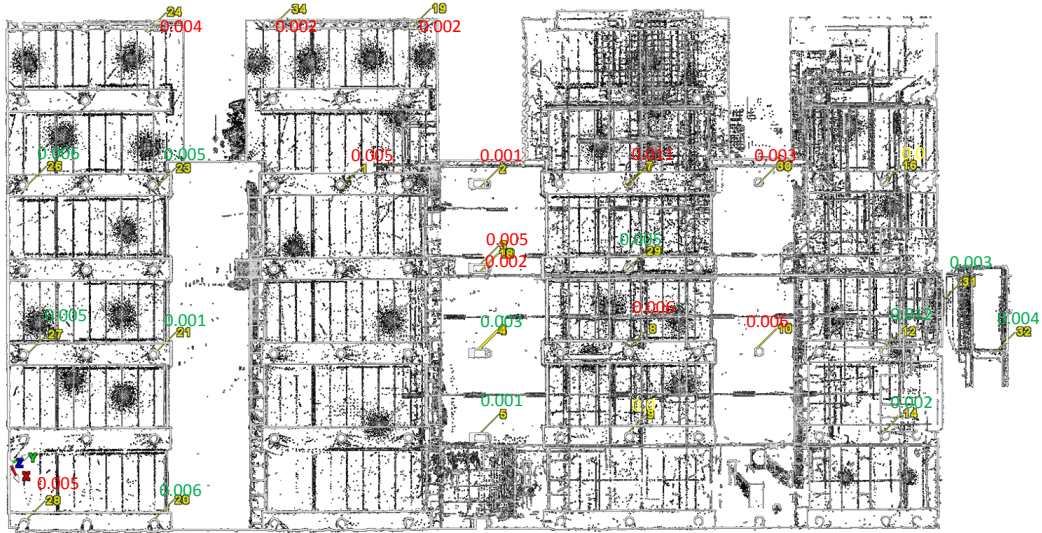
Figure 10: Floorplan with deviations per point. Green indicates the point cloud is above the control points. Red indicates the point is below. All measurements are depicted in [m].
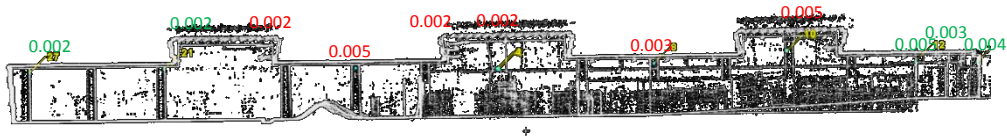

Figure 11: Side view with mean deviations in section view. Green indicates the point cloud is above the control points. Red indicates the point is below. All measurements are depicted in [m].

The cause of the increased error in z direction can be explained by the project geometry. In x and y directions, data distribution reaches up to several tens of meters. In z direction however, the data distribution is only several meters. This causes the registration algorithms to produce a larger amount of uncertainty in the matching. Also, data in the z-direction generally concentrates around 2 areas: The floor and the ceiling. These surfaces are often scanned under a high angle of incidence, resulting in less accurate data. Therefore, due to their specific geometry, these types of AEC industry buildings will be prone to errors in z-direction. Given the mean deviations at varying distances, a deviation model can be calculated for the project (figure 12). A quadratic function is best fitted on the data. This bending model indicates that an error of 0.004m can be expected on a 70m long project.
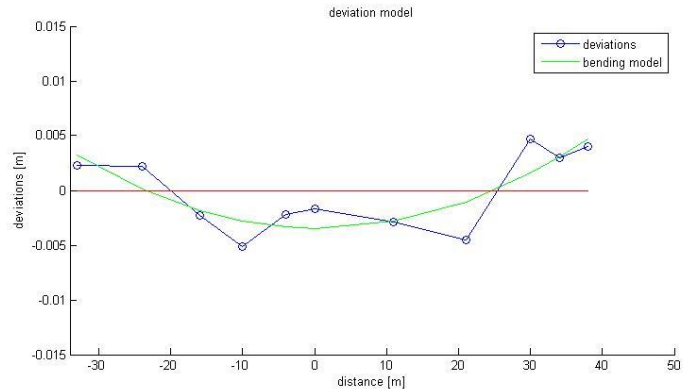
Figure 12: Deviation model base on project data

Given the calculated model, a prediction can be made for other projects (figure 13). The predicted project length for a maximum registration error of 0.015m is approximiatly 150m. However, one should notice that the expected error is highly dependant on de variance of scan data in z-direction.
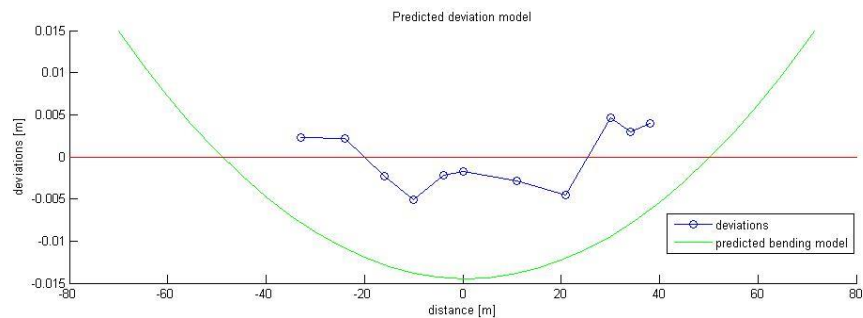

Figure 13: Predicted deviation model base on project data

Large-scale test site

The large-scale test site is the C-pier in Schiphol International Airport. It roughly consists of a long small y-shaped structure of 250 x 100 x 10m (figure 14). Project deliverables also prescribe an overall point cloud accuracy of LOA30 [3]. A reference network was established by an external surveying company using total station measurements.
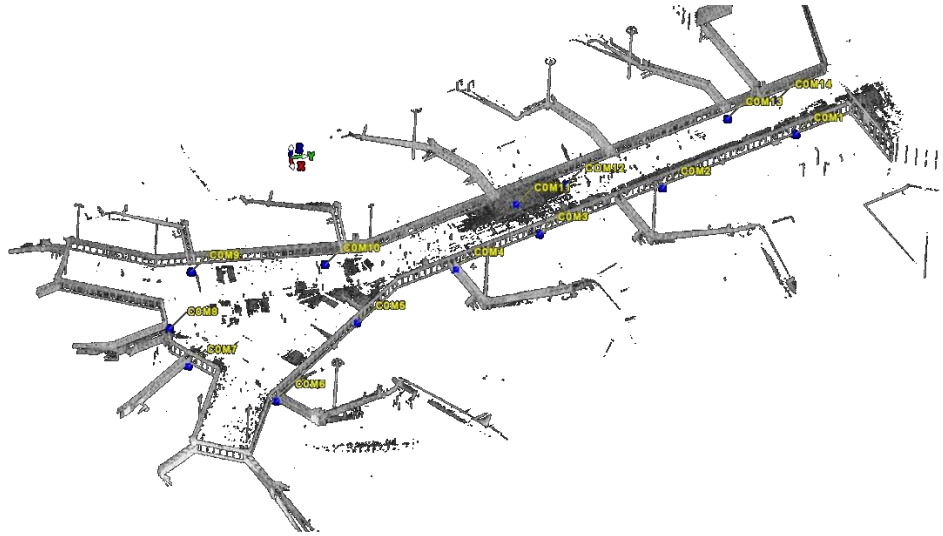
Figure 14: Large data set overview, control points

Data acquisition and processing

Similar like the first test, 422 scans were acquired in the project, resulting in a total point cloud of approximately 3.6 billion points. The site was scanned under 16 hours. 421 manual constraints had to be provided, after which 4900 constraints were automatically found. 30 hours of post-processing was timed, including 10 hours of manual labor.

The control measurements were conducted by a two man team. 146 targets were materialized on the exterior of the scene, providing an accuracy of 2mm on each point. Acquisition and processing was performed in three days.

Comparison

An analogue comparison between both workflows shows that the proposed workflow again is 30% faster (table 4). Similar cost were noted on this project.

	Acquisition time [h]	Post processing [h]	Total [h]
Traditional workflow			
• Point cloud acquisition	16	30	46
• Total station measurements	16	5	21
• GPS	3	1	4
Proposed workflow			
• Point cloud acquisition	16	30	46
• GPS	3	1	4
Saved Time	**16**	**5**	**21**
Efficiency	**46%**	**14%**	**30%**

Table 4: Comparison of both workflows in terms of acquisition speed and post-processing time

To evaluate of the accuracy for this project, 12 targets are monitored during 2 stages. The first stage only considering the cloud to cloud registration, and the second considering the integration of GPS data to improve accuracy. Table 5 shows the results of the cloud to cloud registration compared to the control points. The average deviation in x and y direction is only a few millimeters. Just as the prediction deviation model expected, the error in z exceeds project specifications. A maximum error of 3.71cm is measured at the end of the project. By plotting the deviations on the point cloud, it is revealed that the project again is bending upwards (figure 15).

	X	Y	Z
% within specification (1.5cm)	100%	100%	64%
Biggest error [m]	0,0117	0,0107	0,0371
RMSE [m]	0,0052	0,0040	0,0174

Table 5: Comparison between cloud to cloud registration and the survey network second test case
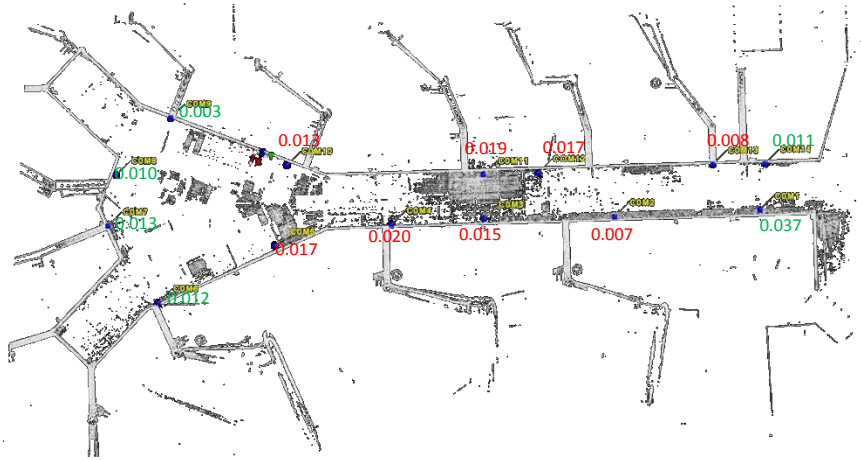
Figure 15: Floorplan with deviations in z per point. Green indicates the point cloud is above the control points. Red indicates the point is below. All measurements are depicted in [m].
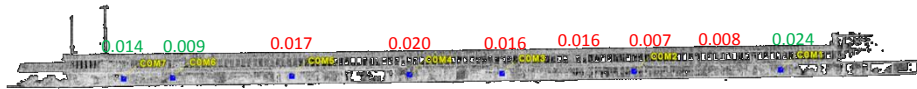

Figure 16: Side view with mean deviations in section view. Green indicates the point cloud is above the control points. Red indicates the point is below. All measurements are depicted in [m].

Given the mean deviations at varying distances (figure 16), the deviation model can be calculated for the project (figure 17). This model indicates that an average error of 2.1cm can be expected on a 220m long project. Given the total length of nearly 270m of the C pier, mean deviations up to 3.7cm are expected.
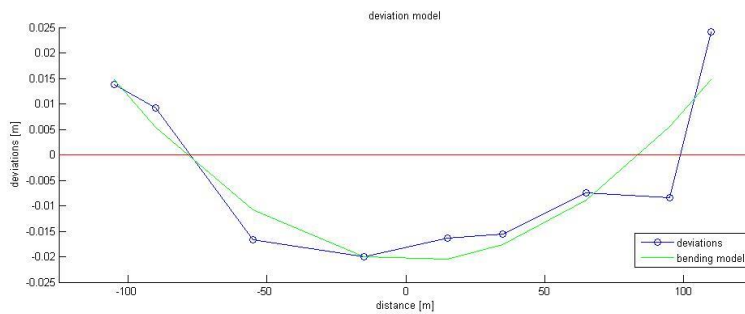

Figure 17: Deviation model base on project data (C-Pier)

Bending model comparison

Comparing this model to the prediction of the first test case, results are differing. Figure 18 shows that the predicted error at varying project lengths will exceed project specifications at a smaller length for the first test case. The explanation can be found in the variance of the data in z-direction. Depending on the variance, the bending angle will differ. The bending angle is inversely proportional to the data variance (figure 18).
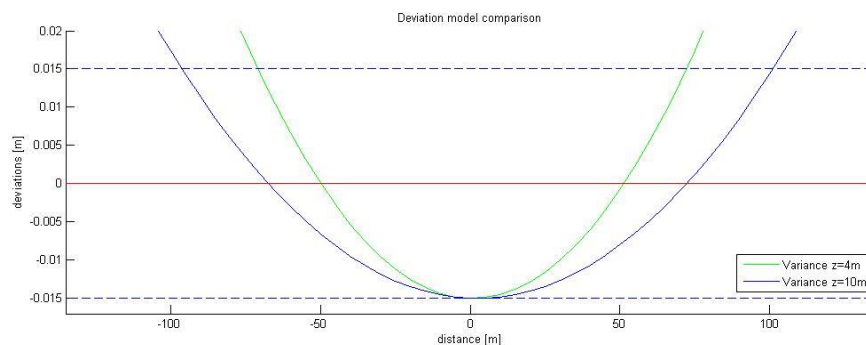

Figure 18: Deviation model comparison for varying data variance. The green curve represents bending prediction for a distribution of 4m, the blue curve for a distribution of 10m

Given these prediction models, an estimation can be made for future projects. E.g. most office buildings have a floor height between three and four meters. Looking at the deviation model, it is estimated that project bending will exceed 1.5cm after approximately 150m. Therefore, 22,500 m² can be scanned before any control should be added.

GPS integration comparison

To improve project accuracy, GPS measurements are integrated. A total of six points were measured in proximity of the project (figure 19). The measurements were acquired using a Trimble R10 [38]. 180 measurements were taken on each point, providing an accuracy of 1.5cm. By scanning the GPS locations, the GPS measurements can be related to be project using cloud to cloud registration.
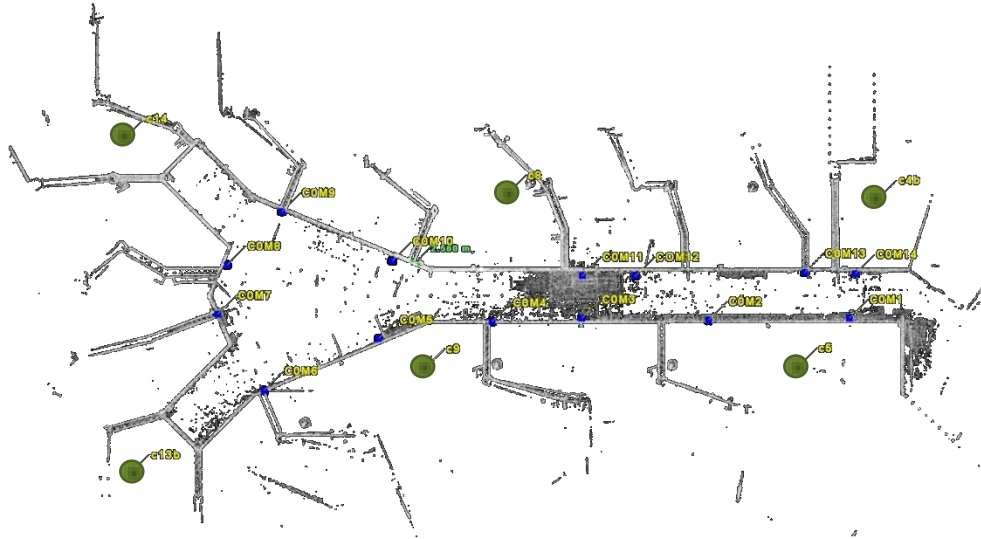
Figure 19: Overview GPS points in project

Table 6 shows the overall accuracy of the GPS integrated registration compared to the control network. The accuracy in x and y direction remains unmodified by the GPS measurements. However, the data in z-direction is optimized and is now within target specifications. Analyzing the deviations reveals that the project bending can be successfully minimized using control points in proximity of the project (figure 20, 21, 22).

	X	Y	Z
% within specification (1.5cm)	100%	100%	100%
Biggest error [m]	0,0140	0,0126	0,0149
RMSE [m]	0,0067	0,0051	0,0071

Table 6: Comparison between GPS integrated cloud to cloud registration and the survey network second test case
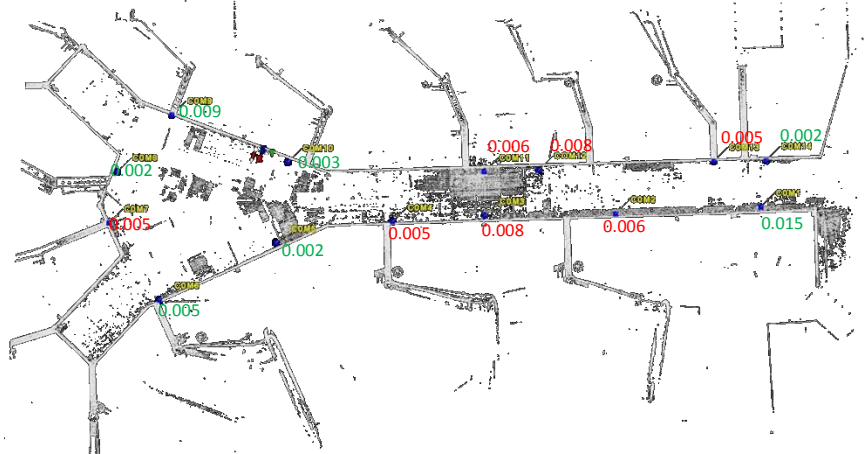
Figure 20: Deviations in z per point. Green indicates the point cloud is above the control points. Red indicates the point is below. All measurements are depicted in [m].

Figure 21: Mean deviations in section view. Green indicates the point cloud is above the control points. Red indicates the point is below. All measurements are depicted in [m].
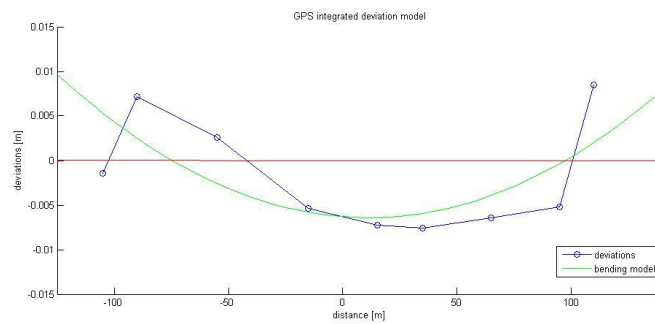

Figure 22: GPS integrated bending model

6. Conclusion

While several systems have been developed over the years, terrestrial laser scanning still has the edge in accuracy and consistency. Also the range, multidisciplinarity and capability to capture RGB are major benefits to the system. However, the workflow is expensive and time consuming. Therefore, a revised workflow is proposed using only a terrestrial laser scanner and GPS measurements. Experimental results show that the new workflow greatly reduces acquisition time and cost. Increases in speed of 39% have been noted.

Using cloud to cloud registration, we believe LOA30 can be met without additional control. Test results prove that the overall accuracy of the registration is within specifications for projects up to hundreds of meters, depending on the data variance. For projects with poor geometry or large data sets (400+ scans), GPS measurements can be used to enhance the registration. Overall, we can conclude that, combined with the proposed workflow, terrestrial laser scanning is currently the best solution for Scan-to-BIM applications.

However, dynamic data acquisition devices are evolving fast. Their capability of rapidly capturing data in real time with several centimeters accuracy already makes these systems employable in a wide scale of applications. Systems like NavVis, that combine multiple sensors, have great potential for mapping applications.

References

[1]   BIMFORUM, "Level of development specification version 2013," pp. 0–124, 2013.

[2]   F. G. D. Committee, "Geospatial Positioning Accuracy Standards PART 4 : Standards for Architecture , Engineering , Construction (A / E / C) and Facility Management," 2002.

[3]   U. S. I. of B. DOCUMENTATION, "USIBD Level of Accuracy (LOA) Specification Guide. Document C120tm [Guide] vers. 1.0," 2014.

[4]   D. J. B. D. Backes, C. Thomson, "Chadwick GreenBIM," 2014.

[5]   C. Thomson, G. Apostolopoulos, D. Backes, and J. Boehm, "Mobile Laser Scanning for Indoor Modelling," *ISPRS Ann. Photogramm. Remote Sens. Spat. Inf. Sci.*, vol. II–5/W2, no. November, pp. 289–293, Oct. 2013.

[6]   T. Whelan, H. Johannsson, M. Kaess, J. J. Leonard, and J. Mcdonald, "Robust Real-Time Visual Odometry for Dense RGB-D Mapping," 2011.

[7]   T. Whelan, M. Kaess, M. Fallon, H. Johannsson, J. Leonard, J. Mcdonald, and J. J. Leonard, "Computer Science and Artificial Intelligence Laboratory Technical Report Kintinuous : Spatially Extended KinectFusion," 2012.

[8]   T. Whelan, H. Johannsson, M. Kaess, J. J. Leonard, and J. Mcdonald, "Robust real-time visual odometry for dense RGB-D mapping," *... (ICRA), 2013 IEEE ...*, no. i, 2013.

[9]   F. T. Ramos, J. Nieto, and H. F. Durrant-Whyte, "Recognising and modelling landmarks to close loops in outdoor SLAM," *Proc. - IEEE Int. Conf. Robot. Autom.*, no. April, pp. 2036–2041, 2007.

[10]   M. Pirovano, "Kinfu – an open source implementation of Kinect Fusion + case study : implementing a 3D scanner with PCL," no. October 2011, 2012.

[11]   H. Du, P. Henry, X. Ren, M. Cheng, D. B. Goldman, S. M. Seitz, and D. Fox, "Interactive 3D modeling of indoor environments with a consumer depth camera," *Proc. 13th Int. Conf. Ubiquitous Comput. - UbiComp '11*, p. 75, 2011.

[12]   F. Steinbrücker, C. Kerl, J. Sturm, and D. Cremers, "Large-Scale Multi-Resolution Surface Reconstruction from RGB-D Sequences," *vision.in.tum.de*, 2013.

[13]   H. Yue, W. Chen, X. Wu, and J. Liu, "Fast 3D modeling in complex environments using a single Kinect sensor," *Opt. Lasers Eng.*, vol. 53, pp. 104–111, Feb. 2014.

[14]   C. Wen, L. Qin, Q. Zhu, C. Wang, and J. Li, "Three-Dimensional Indoor Mobile Mapping With Fusion of Two-Dimensional Laser Scanner and RGB-D Camera Data," vol. 11, no. 4, pp. 843–847, 2014.

[15]   Viametris, "indoor Mobile Mapping System The Freedom to map while in motion," 2007.

[16] M. Bosse, R. Zlot, and P. Flick, "Zebedee: Design of a Spring-Mounted 3-D Range Sensor with Application to Mobile Mapping," *IEEE Trans. Robot.*, vol. 28, no. 5, pp. 1104–1119, Oct. 2012.

[17] R. Zlot, M. Bosse, K. Greenop, Z. Jarzab, E. Juckes, and J. Roberts, "Efficiently capturing large, complex cultural heritage sites with a handheld mobile 3D laser mapping system," *J. Cult. Herit.*, pp. 1–9, Dec. 2013.

[18] B. R. Zlot, M. Bosse, T. Wark, P. Flick, and E. Duff, "CSIRO : Moving Mobile," vol. 2, no. 4, pp. 2–5, 2012.

[19] T. Liu, M. Carlberg, G. Chen, J. Chen, J. Kua, and A. Zakhor, "Indoor Localization and Visualization Using a Human-Operated Backpack System," no. September, pp. 15–17, 2010.

[20] G. Chen, J. Kua, S. Shum, and N. Naikal, "Indoor localization algorithms for a human-operated backpack system," *3D Data Process. Vis. Transm.*, 2010.

[21] P. Tang, D. Huber, B. Akinci, R. Lipman, and A. Lytle, "Automatic reconstruction of as-built building information models from laser-scanned point clouds: A review of related techniques," *Autom. Constr.*, vol. 19, no. 7, pp. 829–843, Nov. 2010.

[22] T. Whelan and M. Kaess, "Deformation-based loop closure for large scale dense rgb-d slam," *IEEE/RSJ Intl. Conf. …*, 2013.

[23] Y. Furukawa, B. Curless, S. M. Seitz, and R. Szeliski, "Reconstructing building interiors from images," *Comput. Vision, 2009 IEEE 12th Int. Conf.*, 2009.

[24] R. B. Roth and J. Thompson, "PRACTICAL APPLICATION OF MULTIPLE PULSE IN AIR (MPIA) LIDAR IN LARGE-AREA SURVEYS," 2007.

[25] M. Kirchhof, B. Jutzi, and U. Stilla, "Iterative processing of laser scanning data by full waveform analysis," *ISPRS J. Photogramm. Remote Sens.*, vol. 63, no. 1, pp. 99–114, Jan. 2008.

[26] L. Geosystems, "Leica AHAB Chiroptera II Topographic & Bathymetric LiDAR System," 2014.

[27] Optech, "Optech Titan Multispectral Lidar System."

[28] P. Van Oosterom, S. Ravada, M. Horhammer, O. M. Rubi, M. Ivanova, M. Kodde, and T. Tijssen, "Point cloud data management," no. July, 2014.

[29] S. Laine and T. Karras, "Efficient sparse voxel octrees.," *IEEE Trans. Vis. Comput. Graph.*, vol. 17, no. 8, pp. 1048–59, Aug. 2011.

[30] B. Y. H. Durrant-whyte, T. I. M. Bailey, P. Cheeseman, J. Crowley, and H. Durrant-, "Simultaneous Localization and Mapping : Part I," 2006.

[31]   N. Pouliot, P. Richard, S. Montambault, A. P. Line, and C. Scanning, "LineScout Power Line Robot : Characterization of a UTM-30LX LIDAR System for Obstacle Detection," pp. 4327–4334, 2012.

[32]   M. Bosse, R. Zlot, and P. Flick, "Zebedee: Design of a spring-mounted 3-d range sensor with application to mobile mapping," *Robot. IEEE Trans.*, vol. XX, no. Xx, pp. 1–15, 2012.

[33]   L. Hokuyo Automatic co., "Scanning Laser Range Finder UTM-30LX-EW Specification," pp. 1–7, 2012.

[34]   J. Huang, D. Millman, M. Quigley, D. Stavens, S. Thrun, and A. Aggarwal, "Efficient, generalized indoor WiFi GraphSLAM," *2011 IEEE Int. Conf. Robot. Autom.*, pp. 1038–1043, May 2011.

[35]   Google project tango (2014). *http://www.google.com/ atap/projecttango/*

[36]   NavVis. (2012-2014). *https://www.navvis.com/explore/trolley/*

[37]   Trimble. (2014.). Trimble Indoor Mobile Mapping Solution (TIMMS) *http://trl.trimble.com/*

[38]   Trimble. (2012-2014) TRIMBLE R10 GNSS System. *http://trl.trimble.com/*

[39]   Durrant-whyte, B. Y. H., Bailey, T. I. M., Cheeseman, P., Crowley, J., & Durrant-, H. (2006). Simultaneous Localization and Mapping : Part I.